recovery energy environment economy

2011 CSPG CSEG CWLS Convention

Synthetic Microseismic Files

J. Wong*, P.M. Manning, L. Han, and J.B. Bancroft
CREWES, University of Calgary
*wongjoe@ucalgary.ca

Summary

We have created synthetic microseismic datasets for testing the accuracy of hypocenter location algorithms. 3C microseismograms with sources and receivers embedded in horizontally layered velocity structures were generated either by ray-tracing (RT) and convolution, or by 2D finite-difference (FD) modeling. The RT-modeled seismograms include direct and head-wave arrivals, but no reflected arrivals. The ray-tracing method can approximate some effects of TTI anisotropy in the layers. Traces from FD modeling include reflected as well as direct and head wave arrivals, but they do not include effects due to anisotropy. Gaussian and harmonic noise are added to the synthetic microseismograms to simulate different signal-to-noise levels, and the modeled data are stored in SEG2 format to conform to field-recorded data files.

Introduction

Passive monitoring of microseismic events induced by hydraulic fracturing has been used for many years, but the fundamental problem of locating hypocenters is still plagued by inaccuracies. Different algorithms and processing flows applied to the same dataset often produce radically different estimates of source locations. This is especially true if the acquisition aperture of the recording array is small in angular extent and if the microseismic arrivals are weak compared to the noise.

We have created synthetic microseismic datasets designed for testing different location algorithms such as migration (Chambers et al., 2008), inversion (Wong, 2009; Wong et al., 2010), and back-projection (Han et al., 2010). Since the hypocenter coordinates for the synthetic data are known, the effectiveness and accuracy of different location methods can be evaluated for various recording geometries and noise levels.

The datasets consist of seismic traces created by ray-tracing or finite difference modeling of subsurface sources and receiver arrays. The P and S velocity structures are discrete layers with horizontal boundaries representing geological structures common in many hydraulic fracture projects. Gaussian noise and harmonic noise are added to the synthetic traces to simulate microseismograms with different signal-to-noise levels. The modeled data are stored in files with SEG2 format so that they are consistent with field-recorded data files.

Hypocenter location techniques require accurate relative amplitudes of the x, y, and z components of P wave arrivals in order that the direction cosines of the propagation vector at receivers may be estimated. They also require accurate arrival times of the P and/or S arrival times relative to some reference time that is not the actual time of occurrence t_0 of the associated microseismic event. Our modeling schemes do not yield true absolute amplitudes for the arrivals present on synthetic traces, but the relative amplitudes of the direct P-wave arrivals from a given 3C geophone are accurate, as are the arrival time moveouts of all modes. Figure 1 shows ray-tracing through an isotropic layers velocity model; Figure 2 shows 3C microseismograms synthesized by convolving a designed source wavelet with delta functions at the ray-traced arrival times.

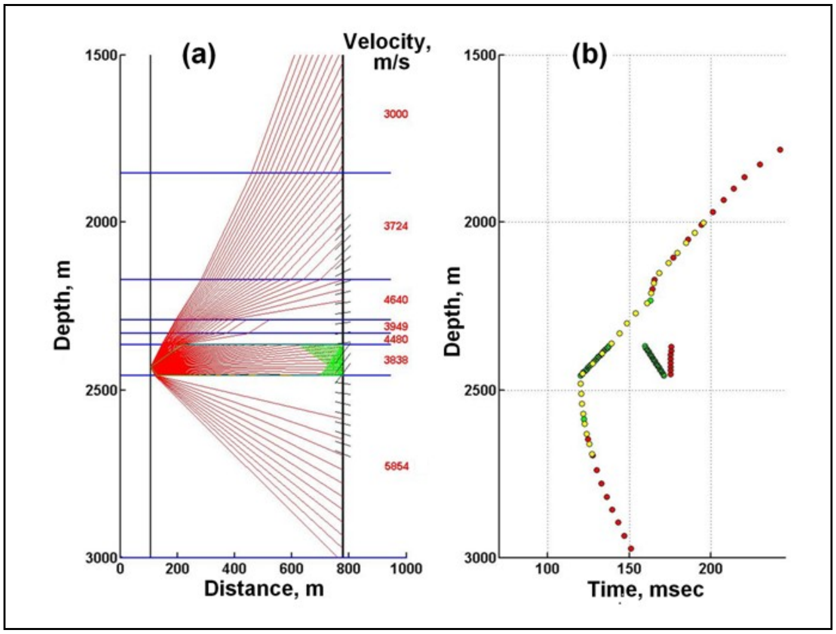

Figure 1: Ray tracing and first-arrival times through a layered isotropic velocity model. Head-wave rays are shown in green; direct-arrival rays are shown in red. Short black lines and yellow dots are propagation directions and arrival times interpolated for specific receiver locations

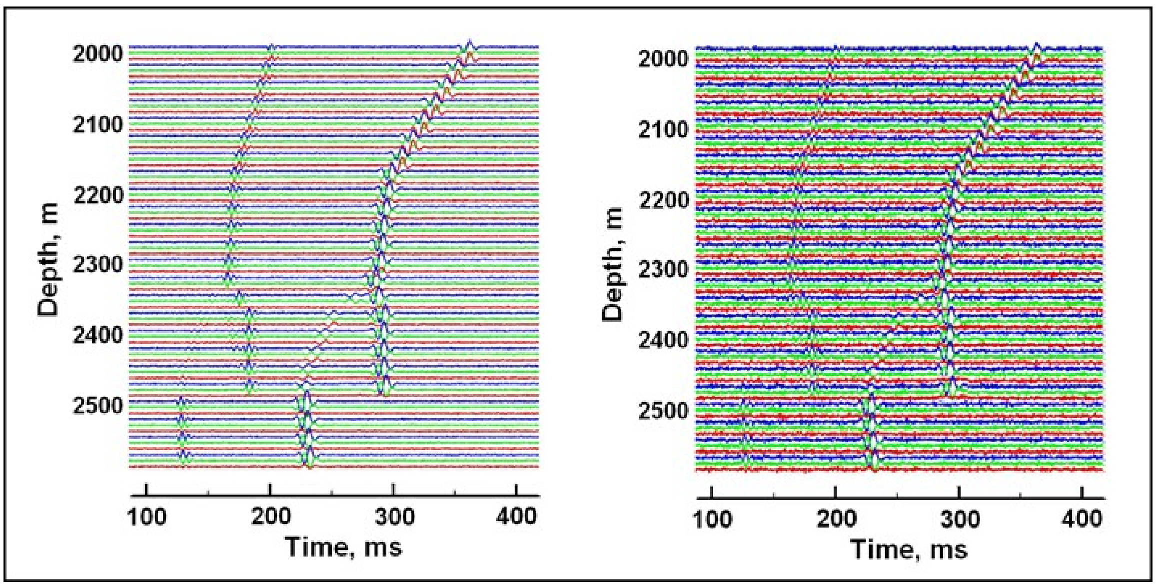

Figure 2: Synthetic microseismograms produced by ray tracing and convolution. The 3C seismograms for each geophone are plotted as a triplet of *x* (blue), *y* (green), and *z* (red) components. Gaussian noise has been added to the clean traces on the left to produce the noisy traces on the right.

Ray Tracing through Anisotropic Layers

Velocity anisotropy often must be accounted for when microseismic monitoring is done in geological environments that include shale layers. We use an approximation developed by Byun et al. (1989) and Kumar et al. (2004) to trace quasi-P (qP) rays through horizontal velocity layers with anisotropy. Microseismograms are then synthesized by convolving the source wavelet with delta functions at the ray-traced direct arrival times for the anisotropic media. The Byun/Kumar approximation for qP group velocities in a VTI medium is given by:

$$V_p^{-2}(\emptyset) = a_0 + a_1 \cos^2\emptyset - a_2 \cos^4\emptyset \ , \quad (1)$$

$$a_0 = V_h^{-2} \ , \quad (2)$$

$$a_1 = 4V_{45}^{-2} - 3V_h^{-2} - V_v^{-2} \ , \quad (3)$$

$$a_2 = 4V_{45}^{-2} - 2V_h^{-2} - 2V_v^{-2} \ . \quad (4)$$

V_v, V_h, andV_{45} are the group velocities in the vertical (Ø=0°), horizontal (Ø=90°), and 45° dip angle directions. For the isotropic case, a_1 and a_1 are identically zero. The VTI symmetry axis can be tilted to simulate TTI (Kumar et al. 2004; Wong, 2010).

Seismograms Produced by 2D Finite Difference Code

Seismograms can also be produced by a 2D time-stepping finite difference (FD) code for isotropic media (Manning, 2007; 2008). FD elastic modeling will automatically generate direct P and S arrivals as well as all the refracted, reflected, and converted arrivals due to the boundaries in the velocity-density model. Because of stability issues related to FD modeling and the desire to have reasonable execution speed and grid array size, we have restricted the dominant frequencies in the synthetic seismograms to be 300 Hz or less. These are low compared to frequencies exceeding 500 Hz commonly observed for microseismic events associated with hydraulic fracturing projects.

Since it is a 2D code, the relative amplitudes and phases of the various arrivals will not be correct for microseismic sources in 3D space, but the kinematics (i.e., arrival times) will be correct. For the direct P arrival, the *x* and *z* amplitudes will be correct in the 2D plane. To simulate the *x* and *y* amplitudes in 3D space, the P-wave *x* amplitudes from the 2D code are split by applying the direction cosines from the source to each receiver. This is a straightforward calculation, since for a horizontally-layered velocity model the projection of the propagation vector between the source and receiver onto the *x*-*y* plane is a straight line.

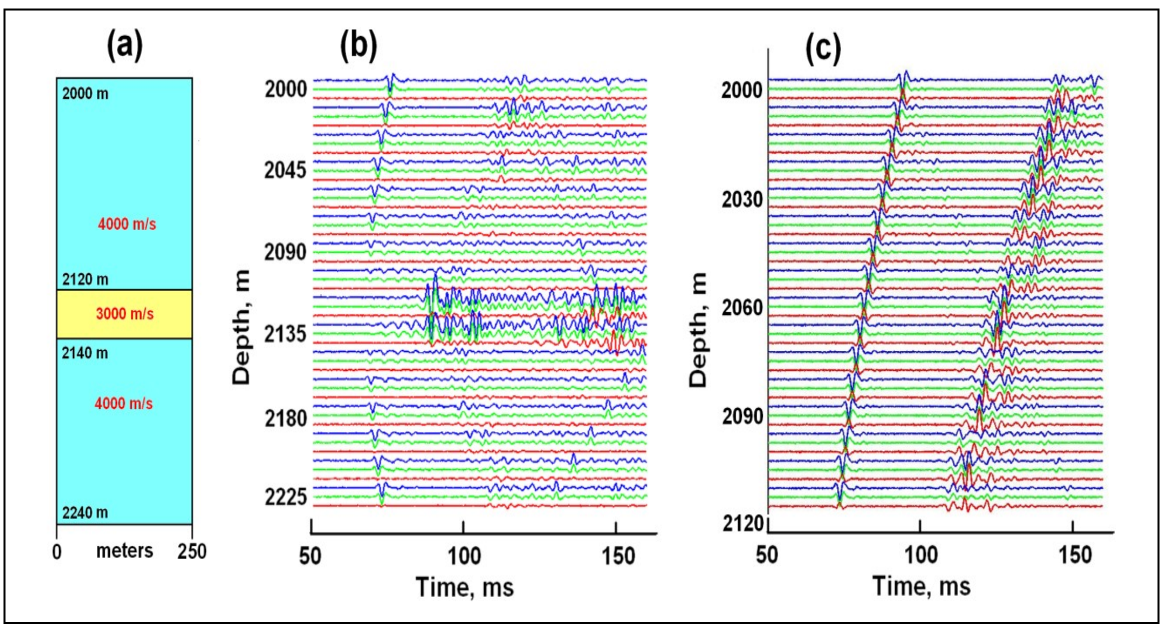

Figure 3: (a) Velocity model for finite difference modeling of microseismograms. A microseismic source is located at $x = 0$ m and depth of 2130 m in the low-velocity layer; (b) seismograms for an array of sixteen 3C geophones straddling the low-velocity zone at x = 250 m; geophone spacing is 15 m; (c) seismograms for an array entirely above the low-velocity zone at $x = 250$ m; geophone spacing is 10 m. Blue, green, red traces are the *x*, *y*, and *z* components, respectively.

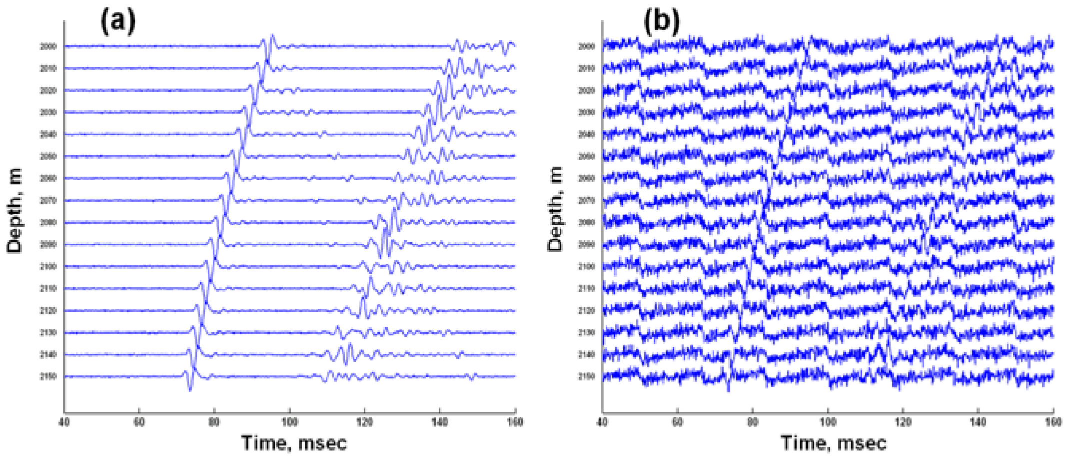

Figure 4: (a) The FD *x*-component microseismograms from Figure 3c with no noise. (b) The same seismograms after 60 Hz harmonic and Gaussian noise are added.

Conclusions

Synthetic three–component microseismograms can be created using either ray-tracing or time-stepping FD modeling through horizontally-layered P and S velocity structures. For the ray-tracing results, the modeled seismograms include only direct and head-wave arrivals, and the velocity model can include VTI or TTI anisotropy in the layers. Traces from FD modeling include reflected and converted as well as direct and head wave arrivals, but they do not include effects due to anisotropy. Gaussian and/or harmonic noise can be added to the synthetic microseismograms to simulate different signal-to-noise levels. The modeled data are stored in SEG2 format to conform to field-recorded data files.

The synthetic data are intended to be used for testing microseismic hypocenter location procedures within hypothetical but realistic geological structures and receiver array configurations. They are suitable only for testing hypocenter location methods that rely on observed arrival times and propagation directions at geophones. They do not contain any information that relate to source mechanisms.

Acknowledgements

This research was supported by the NSERC and the industrial sponsors of CREWES. We thank Jamie Rich of Devon Energy Corporation for providing the velocity model shown on Figure 1.

References

Byun, B.S., Corrigan, D., and Gaider, J.E., 1989. Anisotropic velocity analysis for lithology discrimination: Geophysics, **54**, 1566-1574.

Chambers, K., Brandsberg, S., Kendall, J.M., and Rueda, J., 2008. Testing the ability of surface arrays to locate microseismicity: 78th Ann. Int. Meeting, SEG, Expanded Abstracts, 1436-1439.

Han, L., Wong, J., and Bancroft, J.C., 2010. Back propagation analysis for hypocenter location: CREWES Research Report **22**, 31.1-31.9.

Kumar, D., Sen, M.K., and Ferguson, R.J., 2004. Traveltime calculation and prestack depth migration in tilted transversely isotropic media: Geophysics, **69**, 37-44.

Manning, P.M., 2008. Techniques to enhance the accuracy and efficiency of finite-difference modeling for the propagation of elastic waves: Ph.D. Thesis, University of Calgary.

Manning, P.M., 2008. Finite-difference elastic modeling in MATLAB, workbench version: CREWES Research Report, **20**, 24.1-24.10.

Wong, J., 2009. Microseismic hypocenter location using nonlinear optimization: CREWES Research Report, **21**, 73.1-73.14.

Wong, J., 2010. Fermat's principle and ray tracing through anisotropic layered media: CREWES Report **22**, 88.1-88.9.

Wong, J., Han, L., and Bancroft, J.C., 2010. Microseismic hypocenter location using nonlinear optimization: 80th Ann. Int. Meeting, SEG, Expanded Abstracts, 2186-2190.